

## Force, pressure and strain measurements for traditional heavy mortar launch cycle

Juha Toivola, Seppo Moilanen and Henna-Riitta Jussila

**Summary.** The measurement applications of pressure, forces and strains for traditional heavy mortar launch cycle are presented. Especially the processing method of measured strain data for launch loading determination is discussed. The chamber pressure estimates calculated from measured tube strains are evaluated and the pressure calculation method including compensation of thermal stress proved to be relevant for the case of traditional mortar launch cycle. The transversal component of socket force proved to be insignificant compared to the axial force component. The ground base type had negligible effect on measured socket forces and on extreme base plate strains in this study.

*Key words:* mortars, mortar tubes, mortar base plates, strain gages, force measurement, pressure measurement, strain measurement, test firings

### Introduction

The definitions of pressure terms and their relationship for large caliber weapon systems are presented in standard [1]. The main component of mortar launch loading is a gas pressure of burning propellant charge during internal ballistic cycle of shot.

Traditional methods of gas pressure measurement of heavy guns are mechanical crusher gauge and piezoelectric pressure transducer [2]. The crusher method is based on the measurement of the deformation of copper element due to the pressure resultant force on the piston of crusher gauge. The crusher method gives an estimate of peak gas pressure of shot in gun chamber. The accuracy of estimated crusher pressure value is a function of the shape of pressure curve  $p(t)$ , the type of used crusher gauge and dynamical material properties of crusher element. Some tailored calibration methods have to be used to guarantee the required accuracy of measurement results for crusher method, as shown in Refs. [3] and [4]. Also the construction of the weapon can cause differences in the results of crusher pressures due to the chamber volume, tube dimensions and their effects on the burning rate of propellant charge and the dynamical deformation of crusher element, as shown in Ref. [7].

The piezoelectric pressure transducer gives a pressure vs. time curve  $p(t)$ . High sampling rate and reliability of calibration of transducer can guarantee the high accuracy of pressure peak determination for launch pressure [9] and [10]. The pressures measured by piezoelectric transducers are supposed to be exact values of pressure, but some accuracy problems in calibration still exist especially in cases of high pressure levels and pressure wave determination in gun applications, as discussed in Ref. [8]. The

drawback of piezoelectric transducer is that some kind of mechanical housing (drilling and tapping) for transducer should be machined into the weapon, which cause structural weaknesses and prevent the service use of pressure test weapons. The third pressure measurement method is a combination of crusher and piezoelectric methods. The piezoelectric transducer and its electronics are installed in cylindrical metallic body, which can be put into gun chamber and used like a traditional crusher gauge. Nowadays the sizes of piezoelectric crusher gauges allow their use also in mortar chambers as pressure measurement sensors [11].

The measurement of gun tube strains and strain data analysis offer a reliable comparison method for ballistic pressure measurement. Because the gun tubes are thick wall cylinders with high manufacturing quality (small tolerances in dimensions) and the geometrical changes of shape are usually smooth, the traditional equations of elasticity apply well for deformation vs. pressure load applications [7], [12], [13], [14] and [15]. Special application of tube strain measurement is an evaluation of rotating band loading on gun tubes, which is important for rifled cannon tubes. The application details of band pressure measurements and calculations are discussed in Refs. [16], [17] and [18] and in their sub-references.

During mortar launch cycle the pressure force presses the breech piece towards the base plate and the ground. The value of socket force can be estimated as a resultant force of chamber pressure, but dynamic effects of structures and the stiffness of ground base can cause disturbances on reaction force values. The results of test firing forces and strain measurements can be used as a base of structural designing [19], designing and evaluation of mechanical fatigue laboratory tests and the laboratory acceptance tests of mortar base plate [20].

The modern mortar ammunition can cause higher pressure and force loads due to the increased weight of projectile and higher muzzle velocity than earlier versions of mortar ammunition. The requirements of low weight of weapon construction and good launch stability together with the overall usability of the weapon in all types of ground bases are more or less in conflict with each other.

## **Measurement configuration in mortar test firing**

The purpose of mortar test firing discussed in this paper was to evaluate the socket forces and strains in base plate structure when different kinds of ammunition were fired. Some results of earlier test firings were available in the research report [6], when the base plate was positioned in extreme soft sandy soil or a rigid concrete bed without base plate was used. In this study the ground bases were realistic service cases: Base plate in gravel soil and in sandy soil. The sandy soil ground was created by digging a large cavity in gravel soil and then filling it with sand.

Axial and hoop strains of outside surface of tube chamber section were measured by using biaxial  $0^{\circ}/90^{\circ}$  strain gage rosette. The chamber pressure was calculated from the measured strain data. Direct pressure measurement method was aimed to be used for overpressure rounds by using piezoelectric pressure transducer, but the measurement failed.

Special breech piece with dog-bone geometry was used for socket force measurement, when service rounds or equivalent rounds were fired. The cylindrical part of the breech piece body was instrumented as a force transducer by tri-axial strain gage rosettes as shown in figure 1. Finally the base plate was also instrumented by strain gages. The positions of strain gages are shown in figure 2.

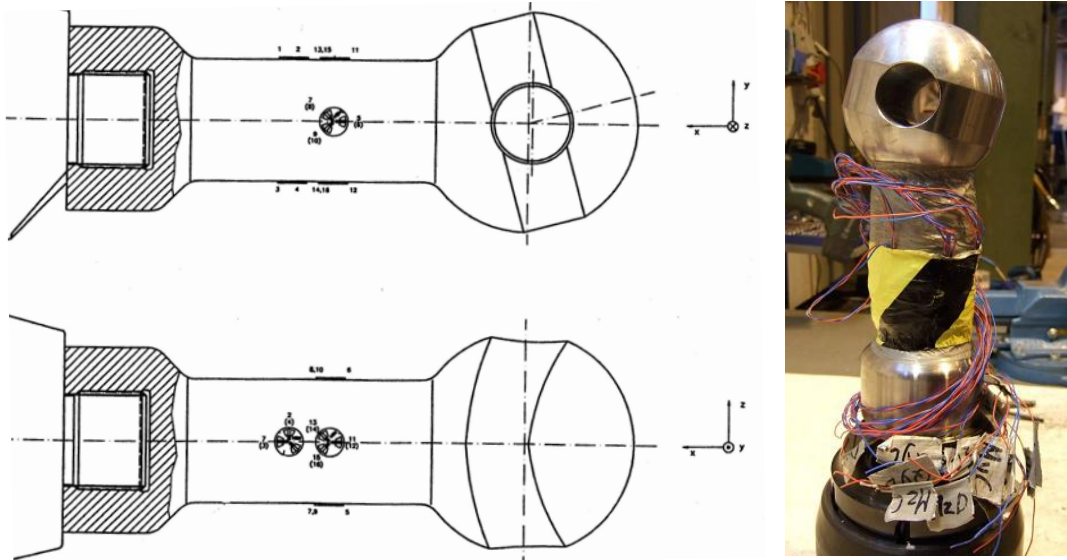


Figure 1. Special breech piece for socket force measurement. Strain gage instrumentation [5] and real structure.

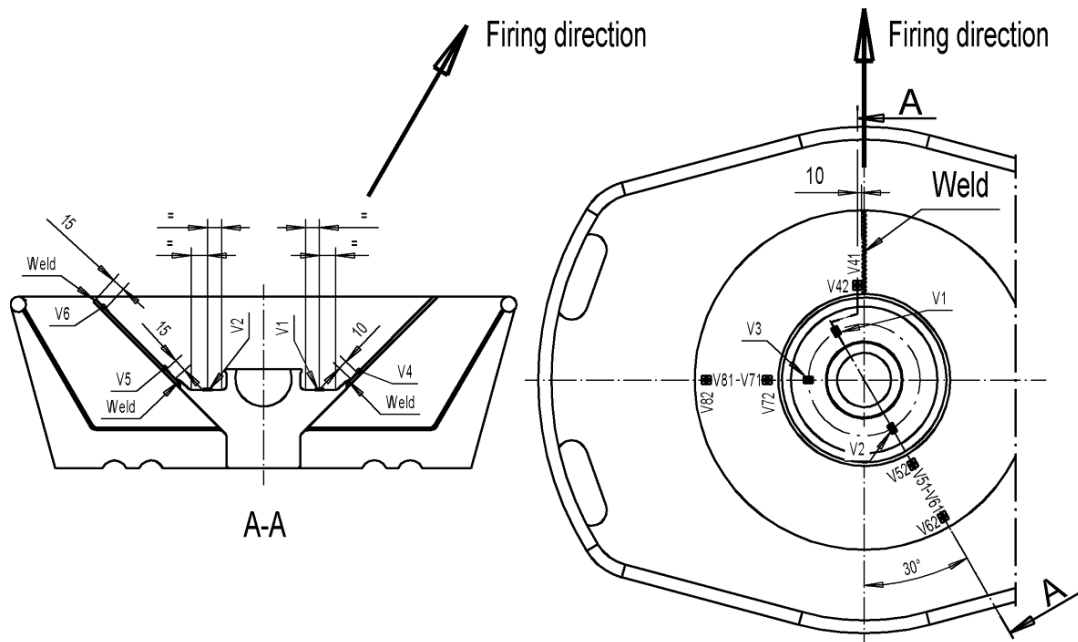


Figure 2. Strain gage positions on base plate

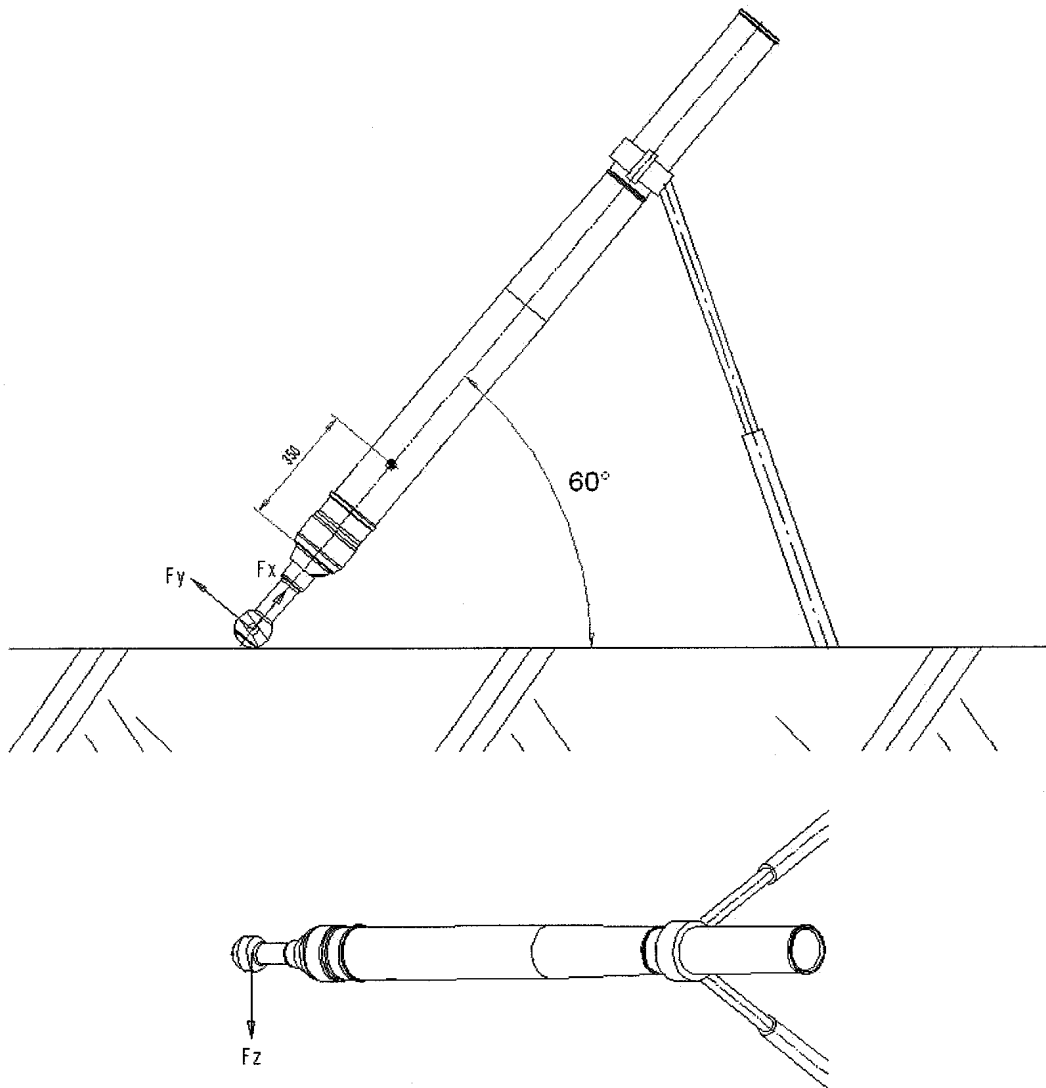


Figure 3. Socket forces acting on instrumented breech piece, base plate is not shown. Strain gage rosette for pressure measurement located on chamber section of tube, distance of 350 mm from tube base end.

### *Test weapon and ammunitions*

Test weapon was Finnish 120 KRH 92 mortar (Patria 120 mm long range mortar) with special force measurement breech piece. The projectiles used in tests were traditional 120 mm HE mortar shell (projectile mass  $m_p \approx 13$  kg) and 120 mm ballistic slug (projectile mass range  $m_p = (15 \dots 20)$  kg). Different charge zones from low pressures up to overpressure levels were used. The weapon and examples of used ammunition types are shown in figures 4 and 5, respectively.

Totally 34 rounds were fired in test including:

- $4 + 4 + 2 = 10$  warmers and base plate stabilizing rounds
- $3 + 5 + 8 = 16$  service rounds
- $3 + 5 = 8$  pressure control and overpressure rounds on sandy soil.



Figure 4. Traditional muzzle loaded 120 KRH 92 mortar on gravel soil before firing. The main components of mortar are: Base plate, special breech piece for socket force measurements, tube, sight unit and bipod assembly.



Figure 5. Traditional 120 mm HE shells (left) and ballistic slugs (right) with charge modules.

### *Measurement hardware*

The hardware of measurements was:

- Strain gages on base plate and tube;
  - Kyowa KFG-5-120-C1-11L3MR,  $k=2.10$ , uniaxial
  - Kyowa KFG-2-120-D16-11L5M3S,  $k=2.06$ , biaxial  $0^\circ/90^\circ$  rosette
  - Kyowa KFG-5-120-D16-11L5M3S,  $k=2.06$ , biaxial  $0^\circ/90^\circ$  rosette.
- Strain gages on force measurement breech piece;
  - HBM RY31 6/120,  $k=1.93$ , tri-axial  $0^\circ/45^\circ/90^\circ$  rosette.
- Kistler piezoelectric pressure transducer K 6215 (used for overpressure rounds)
- PCB charge amplifier 422D13/A (used for overpressure rounds)

- IOtech Wavebook Data Acquisition Unit
- IOtech WBK 16 Strain Gage Signal Conditioner
- LapTop PC Computer
- Weibel W-700M Velocity Analyzer
- Citius C10 and C100 Centurio high speed video cameras
- Zwick/Z250 tensile test machine for calibrating of axial force of breech piece for socket force measurement
- Tamtron MCS 0-6300 kg electronic scale for calibrating of transversal socket forces of breech piece.

Sampling rate  $f_s=40$  kHz was used in measurements and totally 20 channels were used for strain and force measurements:

- 5 channels for socket forces measurements;
  - 1 full bridge for axial force  $F_x$
  - 2 full bridges for transversal forces  $F_y$  and  $F_z$  (shear deformation)
  - 2 half bridges for transversal forces  $F_y$  and  $F_z$  (bending deformation).
- 15 channels for strain measurement ( $1/4$  bridges);
  - 2 channels of tube strains for pressure measurement
  - 13 channels for base plate strain measurement.

One channel was used for direct chamber pressure measurement by piezoelectric transducer for overpressure rounds, when standard pressure measurement breech piece was used instead of special force measurement breech piece. The later one was originally designed for measurements of the loading level of service round firing.

### *Data analysis software*

The measured data was stored and analysed by using Matlab software.

## **Computation of pressure estimates from measured data**

### *Theoretical basis of pressure computation from strains of tube wall*

Axial and hoop strains were measured at outer surface of tube where axial and hoop stresses arise from following phenomena:

Axial stress:

- tube bending (including bending vibration)
- axial rigid body acceleration (including rigid body vibration of the tube)
- axial elastic vibration
- axial loading by friction between projectile and inner surface of the tube (insignificant in presented case)
- inner surface radial pressure loading variation in axial direction (insignificant in presented case)
- thermal stress due to nonlinear temperature distribution.

Hoop stress:

- inner surface radial loading by projectile (insignificant in presented case)
- inner surface radial loading by gas pressure
- thermal stress due to nonlinear temperature distribution.

Axial stress is denoted as

$$\sigma_a = \sigma_{aB} + \sigma_{aA} + \sigma_{ap} + \sigma_{aT} , \quad (1)$$

where  $\sigma_{aB}$  is bending stress,  $\sigma_{aA}$  axial stress arising from purely axial phenomena (axial acceleration, vibration and loading),  $\sigma_{ap}$  axial stress caused by inner surface radial loading variation in axial direction and  $\sigma_{aT}$  axial stress due to nonlinear temperature distribution. Similarly hoop stress is decomposed as

$$\sigma_\theta = \sigma_{\theta p} + \sigma_{\theta T} , \quad (2)$$

where  $\sigma_{\theta p}$  is hoop stress caused by inner surface radial loadings and  $\sigma_{\theta T}$  hoop stress due to nonlinear temperature distribution. Generalised Hooke's law for plane stress state is

$$\begin{aligned} \varepsilon_\theta &= \frac{1}{E}(-\nu\sigma_a + \sigma_\theta) + \varepsilon_T \\ \varepsilon_a &= \frac{1}{E}(\sigma_a - \nu\sigma_\theta) + \varepsilon_T \\ \varepsilon_T &= \alpha\Delta T , \end{aligned} \quad (3)$$

where  $E$  is Young's modulus,  $\nu$  Poisson's factor,  $\alpha$  temperature expansion coefficient,  $\varepsilon_\theta$ ,  $\varepsilon_a$  and  $\varepsilon_T$  are hoop, axial and thermal strain respectively and  $\Delta T$  change of temperature.

During internal ballistic cycle lasting for some milliseconds, temperature change at outer surface is small. For this reason thermal strain  $\varepsilon_T = \alpha\Delta T$  is neglected in the sequel. For longer measurement time this naturally does not hold and strain gage response curve for thermal strain is needed if this term is kept in analysis (for ideally temperature compensated strain gages response to thermal strain is zero) and temperature should be measured or thermal strain should be compensated by another means.

According to Ref. [21] for stationary case of long axially free cylinder under axisymmetric axially uniform thermal loading it can be shown that axial and hoop stresses at outer surface are equal. In Ref. [21] it has been shown that thermally induced vibrations are prominent for slender beams and thin plates. Based on these classical results, it is assumed that thermally induced vibrations are insignificant and axial and hoop thermal stresses at outer surface are equal, i.e.  $\sigma_{aT} = \sigma_{\theta T} = \sigma_T$ .

Outer surface hoop stress for long open-ended thick wall cylinder under internal uniform pressure is

$$\sigma_\theta = \frac{2p}{\omega^2 - 1} , \quad (4)$$

where  $p$  is the internal pressure,  $\omega = D/d$  the wall ratio,  $D$  the outer diameter of the cylinder and  $d$  the inner diameter of the cylinder. Although assumptions behind equation (4) are not completely fulfilled in the case of gun tube, results and interpretations based on this approach have been found useful.

In order to cancel out some unwanted phenomena from computed results, weighted sum of strain components is written as

$$\varepsilon_\theta + \lambda \varepsilon_a = \frac{1}{E}(1 - \lambda \nu) \frac{2p}{\omega^2 - 1} + \frac{1}{E}(\lambda - \nu)(\sigma_{aA} + \sigma_{aB} + \sigma_{ap}) + \frac{1}{E}(1 - \nu)(1 + \lambda) \sigma_T. \quad (5)$$

It can be seen that by choosing weighting factor  $\lambda = -1$  cancels out thermal stress, but axial phenomena remains. Choosing  $\lambda = \nu$  axial phenomena can be cancelled out, but thermal stress remains. Solving internal pressure for these cases results

$$\lambda = -1: p = \frac{\omega^2 - 1}{2} \frac{E}{1 + \nu} (\varepsilon_\theta - \varepsilon_a) + \frac{\omega^2 - 1}{2} (\sigma_{aA} + \sigma_{aB} + \sigma_{ap}) \quad (6)$$

$$\lambda = \nu: p = \frac{\omega^2 - 1}{2} \frac{E}{1 - \nu^2} (\varepsilon_\theta + \nu \varepsilon_a) - \frac{\omega^2 - 1}{2} \sigma_T. \quad (7)$$

From equations (6) and (7) it is seen, that some error is unavoidable. Choice should be made according to which error seems to be smaller, error caused by thermal stress or error caused by axial phenomena.

According to analysis presented above internal pressure estimates are

$$\lambda = -1: p_1 = \frac{\omega^2 - 1}{2} \frac{E}{1 + \nu} (\varepsilon_\theta - \varepsilon_a) \quad (8)$$

$$\lambda = \nu: p_2 = \frac{\omega^2 - 1}{2} \frac{E}{1 - \nu^2} (\varepsilon_\theta + \nu \varepsilon_a). \quad (9)$$

When left hand side pressures in equations (6) and (7) are taken as real gas pressure, using equations (8) and (9) results

$$p_1 = p - \frac{\omega^2 - 1}{2} (\sigma_{aA} + \sigma_{aB} + \sigma_{ap}) \quad (10)$$

$$p_2 = p + \frac{\omega^2 - 1}{2} \sigma_T, \quad (11)$$

where  $p$  is a real gas pressure. Because thermal stress  $\sigma_T$  is positive at the outer surface, estimate  $p_2$  always overestimates the real pressure.

In the absence of axial phenomena it is possible to estimate thermal stress  $\sigma_T$  at outer surface. Using weighting factor  $\lambda = 1/\nu$  in equation (5) and solving for thermal stress yields

$$\sigma_T = \frac{E}{1 - \nu^2} (\nu \varepsilon_\theta + \varepsilon_a) - (\sigma_{aA} + \sigma_{aB} + \sigma_{ap}). \quad (12)$$

Thermal stress estimate is

$$\sigma_{T,est} = \frac{E}{1 - \nu^2} (\nu \varepsilon_\theta + \varepsilon_a) \quad (13)$$

and it's relationship to true thermal stress  $\sigma_T$

$$\sigma_{T,est} = \sigma_T + (\sigma_{aA} + \sigma_{aB} + \sigma_{ap}). \quad (14)$$



### *Other pressure estimates*

In actual measurements pressure estimate from direct pressure measurement was denoted as  $p_3$  for overpressure rounds. Because the direct pressure measurements using piezoelectric pressure transducer failed, the results of them are not presented.

In this study fourth possibility to estimate tube pressure is to compute it from socket axial force  $F_x$  measurement:

$$p_4 = \frac{F_x}{A}, \quad (15)$$

where  $A$  is a pressurized area of tube cross section.

When socket axial force is assumed to be positive for compressive force and acceleration  $a$  is assumed to be positive towards the rear end of the tube, the equation of motion for the tube assembly is

$$pA - F_x = ma, \quad (16)$$

where  $p$  is a real gas pressure at the bottom of the tube and  $m$  is the mass of tube and breech piece. Combining equations (15) and (16) it is seen that

$$p_4 = p - \frac{ma}{A}. \quad (17)$$

Assuming that axial stress in equation (10) is due to rigid body acceleration,  $\sigma_{aA} = m_t a / A_t$ , and using numerical values for a particular case in hand it is found that

$$p_1 = p - \frac{\omega^2 - 1}{2} \frac{A}{A_t} \frac{m_t}{m} \frac{ma}{A} = p - 0.35 \frac{ma}{A}, \quad (18)$$

where  $A_t$  is the cross sectional area of tube wall at strain measurement point on the tube and  $m_t$  is the partial mass of the tube from the strain gage position to muzzle end.

At the beginning of the internal ballistic cycle acceleration is positive and both estimates  $p_1$  and  $p_4$  underestimate the true pressure. Comparing equations (17) and (18) it is readily seen that error caused by axial rigid body acceleration  $a$  is clearly smaller in estimate  $p_1$  than in estimate  $p_4$  and thus at the beginning of the internal ballistic cycle estimate  $p_1$  should exceed estimate  $p_4$ .

### *Choice for chamber pressure estimate*

For overpressure rounds pressure was intended to be measured using piezoelectric transducer, and strain gages were meant to be a backup pressure sensor if direct pressure measurement fails. Unfortunately this was what happened because of poor charge amplifier action. Therefore direct pressure measurement results for these rounds were doubtful. For service rounds strain gages on the tube surface were intended to act only as pressure measurement sensor, because special force measurement breech piece was used and direct pressure measurement was impossible. This situation necessitated analysis and comparison of different pressure estimators and a choice between them in this study. The comparison of direct pressures with strain pressures is discussed shortly in Ref. [7].

Choice between pressure estimates  $p_1$  and  $p_2$  must be based on measured data and type of weapon. Experience from several measurements of recoiling cannon has shown that acceleration of recoil movement and muzzle brake force is clearly visible in tube

strain measurements and so axial effects need to be compensated. Also rotating band pressure creates axial stress when it passes measurement point as shown in Refs. [16], [17] and [18]. For a traditional smooth bore mortar there is no recoil mechanism, no muzzle brake and no rotating band passing present. Based on these considerations both of pressure estimates ( $p_1$ ,  $p_2$ ) can be chosen for traditional mortar firing.

In figure 6 measured hoop and axial strains are presented for a typical mortar shot. As can be seen there is no significant axial or bending vibration visible after internal ballistic cycle and hence it can be assumed that elastic vibrations are absent. Considering axial effects, only rigid body acceleration and thermal stress could be present. Effect of thermal stress is visible in figure 6 after internal ballistic cycle, where both axial and hoop strain settles rapidly to approximate level of  $50 \mu\text{m/m}$  corresponding to thermal stress of 15 MPa at outer surface. This also proves experimentally, that after internal ballistic cycle both axial and hoop strains and stresses are equal although temperature field is non-stationary.

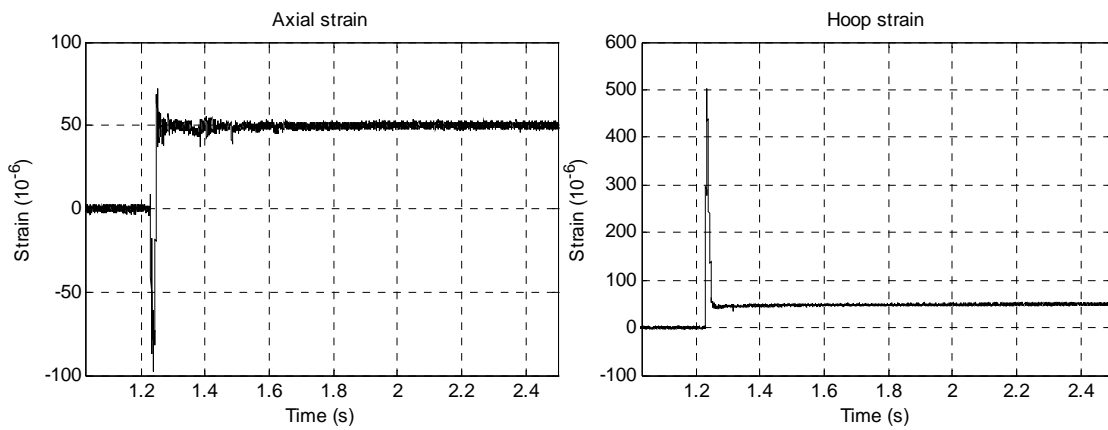


Figure 6. Axial and hoop strain of tube for typical mortar shot.

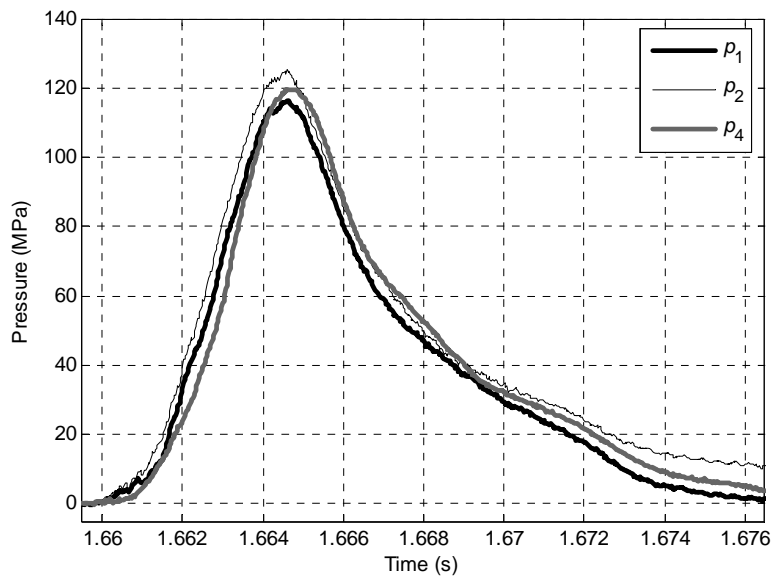


Figure 7. Pressure estimates  $p_1$ ,  $p_2$  and  $p_4$ .

Pressure estimates  $p_1$ ,  $p_2$  and  $p_4$  are shown in figure 7 for a typical service round when the soil base has been compacted by previous rounds. There are several issues visible:

- Estimate  $p_2$ , which is known to overestimate real pressure, always exceeds estimate  $p_1$ .
- Estimate  $p_1$ , which underestimates real pressure less than  $p_4$  when acceleration is positive, exceeds estimate  $p_4$  almost to the pressure peak. When estimates  $p_1$  and  $p_4$  coincide, acceleration changes sign (within the measurement and analysis accuracy).
- Thermal stress, which is the only error source for estimate  $p_2$ , develops very rapidly and has almost reached its final value at pressure peak.
- Estimate  $p_2$  clearly overestimates pressure peak value.
- For this round estimate  $p_1$  probably slightly overestimates pressure peak value.
- For this round estimate  $p_4$  apparently overestimates pressure peak value, because acceleration has changed sign before peak and estimate  $p_4$  (and  $p_1$ ) overestimates the real pressure under negative acceleration (after crossing of estimates  $p_1$  and  $p_4$ ).

Based on the observations above, estimate  $p_1$  seems to be the best choice. Pressure peak value is an important result parameter. Because estimate  $p_2$  always overestimates the real pressure, pressure peak value and also gas impulse computation will be erroneous. For estimate  $p_4$  it is not known in advance whether it overestimates or underestimates pressure peak value because acceleration could change sign before or after pressure peak depending on the characteristics of the soil base.

### *Thermal stress of tube*

In figure 8 typical result for estimated thermal stress together with pressure estimates  $p_1$  and  $p_2$  is shown. After internal ballistic cycle thermal stress rapidly settles to approximate level of 27 MPa for this round. During internal ballistic cycle thermal stress estimate rises almost immediately up to the final level and then drops before climbing up to the final level again. This is because axial acceleration effect is superimposed into the estimate. At the beginning of internal ballistic cycle axial acceleration is positive and hence thermal stress estimate overestimates the real thermal stress (Eq. 14). However, thermal stress builds up very rapidly. At the beginning of the internal ballistic cycle propellant gas temperature is higher due to burning and heat transfer into the tube is efficient. At later part of the cycle propellant gas expands and cools therefore reducing heat transfer.

## **Results**

### *Socket forces vs. pressure*

The socket forces vs. time  $t$  curves together with the pressure  $p_1(t)$  and tube strain curves for service round fired on sandy soil are presented in figure 9. The maximums of force components occurred at the same time as the maximum of gas pressure. The directions of “vertical” transversal force component  $F_y$  are opposite between the

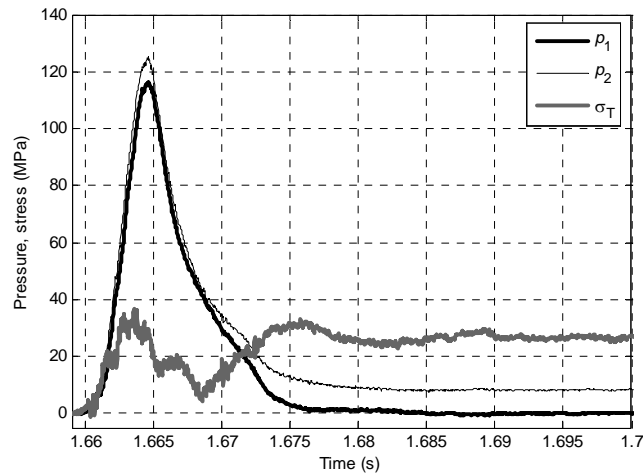


Figure 8. Thermal stress estimate and pressure estimates  $p_1$  and  $p_2$ .

measurement methods (shear or bending). This is supposed to be a consequence of non-symmetric contact between the socket ball of breech piece and socket cup of base plate. Because the maximum values of axial force  $F_x$  are (30...100) times higher than maximums of transversal force components, the small eccentricity in the contact with the socket can cause bending moment due to the axial force. Based on these considerations measurement results relying on shear deformation of dog bone rod were assumed to be a better choice for transversal force estimations.

The maximum value of axial socket force  $F_x$  vs. maximum gas pressure  $p$  is presented in figure 10 for different types of ground and gas pressure range (25...125) MPa. The rounds of earlier work were fired on the extremely soft sandy soil with base plate and on the fixed socket cup on concrete bed without base plate. Previously the special pressure measurement tube had been used and gas pressure had been measured using a piezoelectric pressure sensor mounted on tube wall. The results presented in previous report [6] are included in figure 10.

In earlier work [6] it was shown that:

- The force results of soft sandy soil case were clearly lower than theoretical gas pressure resultant force value  $\max F_x = \max p \cdot A$
- The effect of compaction of soft sandy soil base due to firing can be seen. Stabilising rounds (index A, marker  $\circ$ ) have lowest force value compared to pressure. The forces increased towards to the theoretical line, when the next series (index B and C, marker  $\square$ ) were fired. The force values are even higher for series C (fired after B series round) at lower gas pressure than for the rounds of stabilising series A with higher gas pressure maximums
- The maximum axial forces were  $\sim 30\%$  higher than theoretical gas pressure resultant force when the rounds were fired on fixed socket cup (marker  $\diamond$ ).

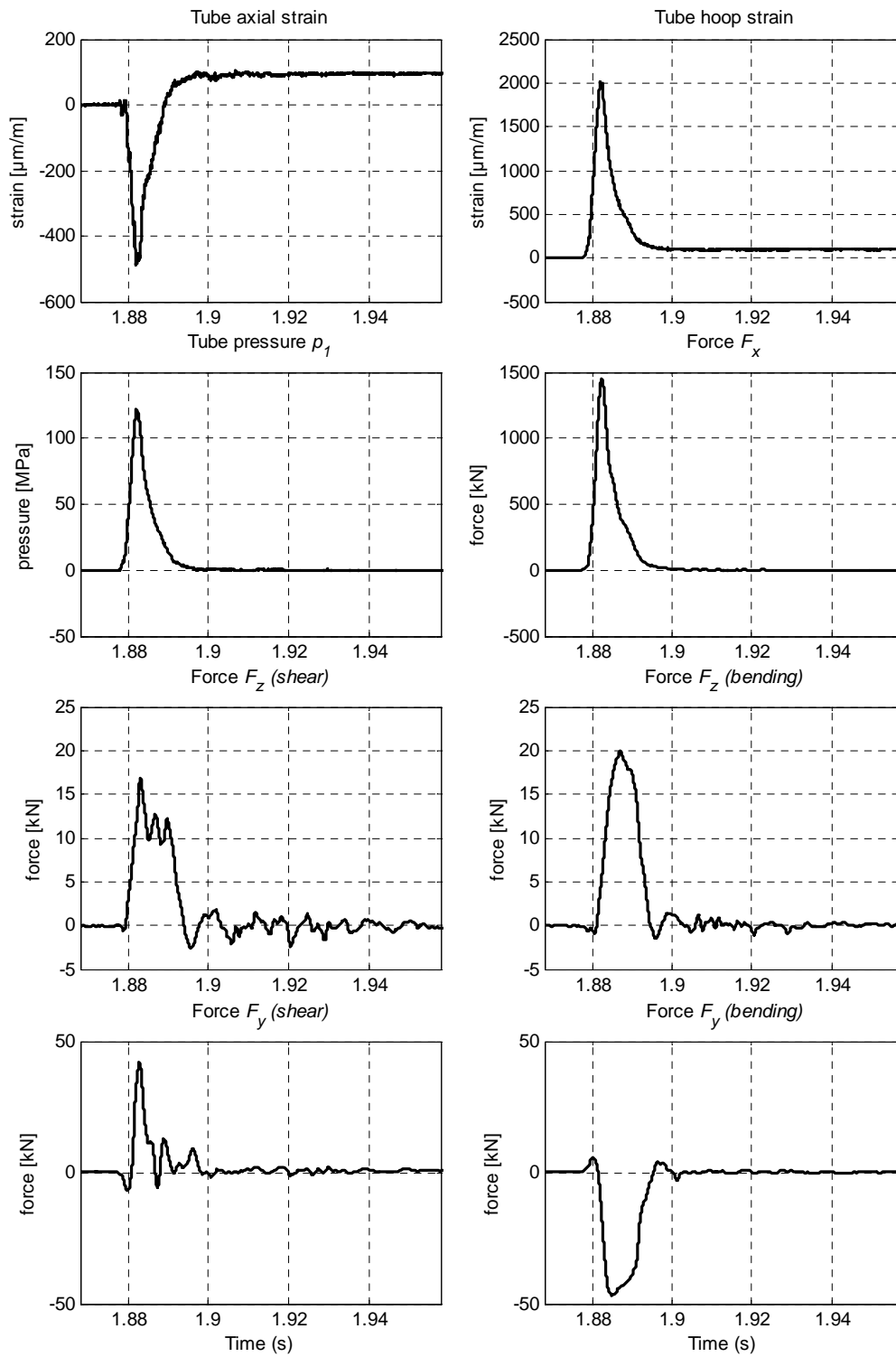


Figure 9. Axial and hoop strain components of tube wall, pressure calculated from strains  $p_1(\varepsilon_x, \varepsilon_\theta)$  and socket forces of the round fired on sandy soil: Axial force  $F_x$ , transversal forces  $F_z$  and  $F_y$  measured by shear and bending deformations.



shown in results of strain gage V42 where strain history is clearly different for sandy and gravel soil base.

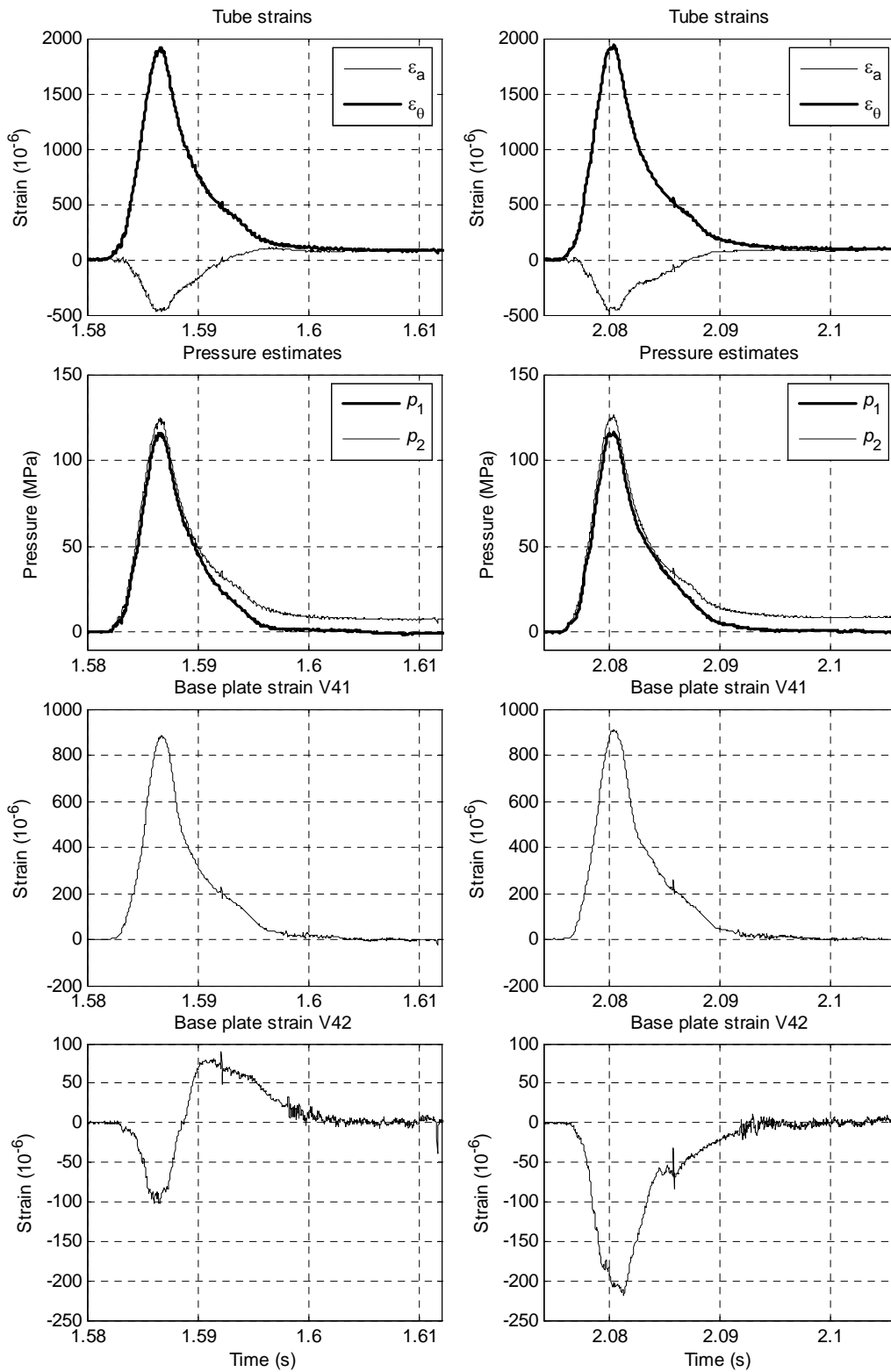


Figure 11. Left column gravel soil, right column sandy soil, service rounds.

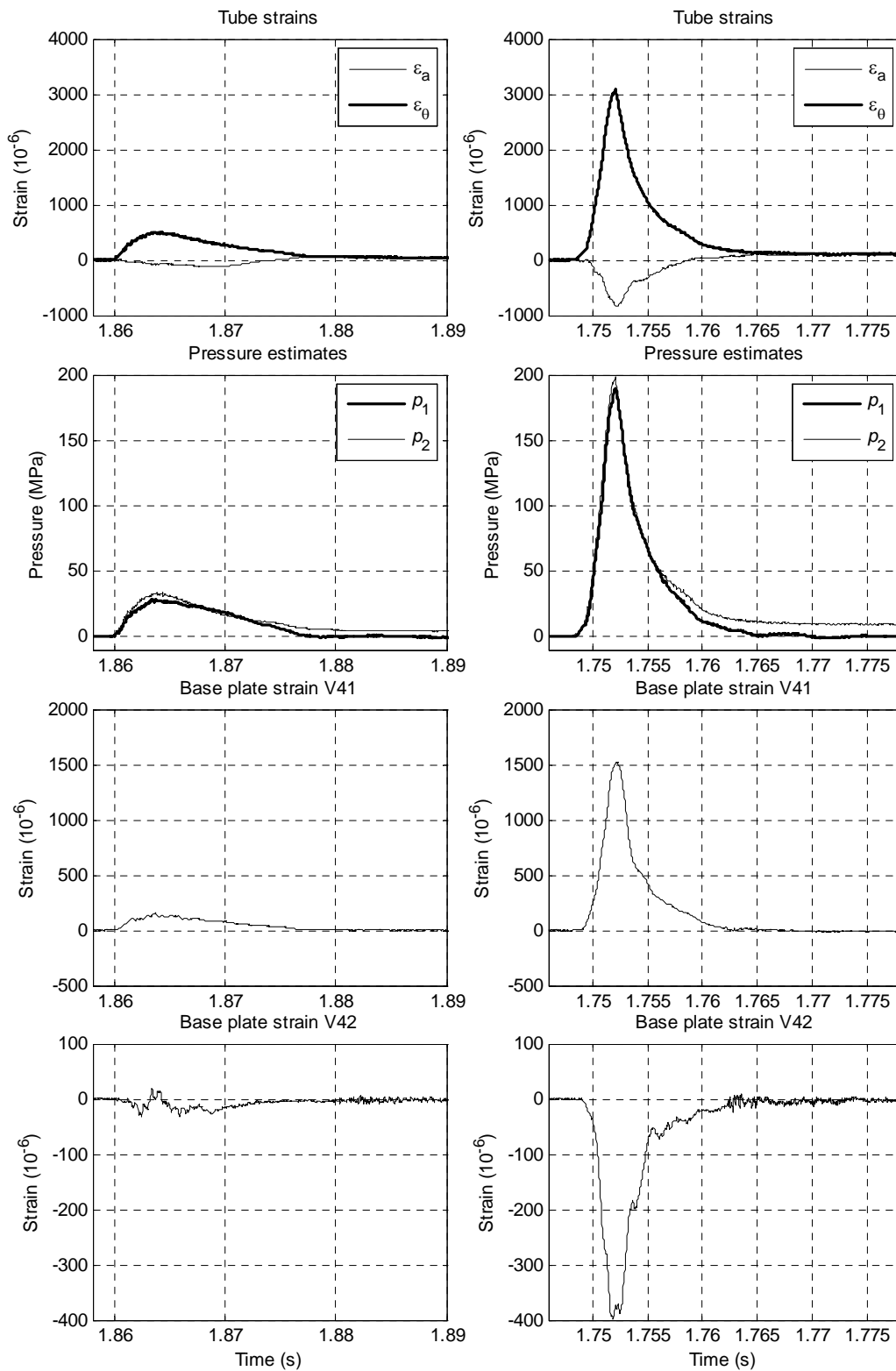


Figure 12. Left column low pressure round, right column overpressure round.



In figure 12 tube strains, pressure estimates  $p_1$  and  $p_2$ , base plate strains V41 and V42 are presented for two extreme rounds, one with low pressure charge and another for overpressure charge. Both rounds were fired on sandy soil. Comparing pressure estimates and base plate strain V41 it is seen that maximum values of base plate strain and tube internal pressure do not follow linear dependence. This is more pronouncedly visible in the results for strain gage V42 where strain response to low pressure round is low but to overpressure round both maximum strain level and overall behaviour of strain history are completely different.



Figure 13. Base plate after service rounds firing on gravel soil (left) and on sandy soil (right).

Table 1. Number of fired rounds in series, pressure estimate  $p_1$ , socket force component  $F_x$  and major limit value of base plate strains for the rounds fired on the gravel base. The mean and standard deviation values are presented for the series including many rounds.

No of rds.	$p_1$	$F_x$	V1	V2	V3	V41	V42	V51	V52	V61	V62	V71	V72	V81 <sup>§</sup>	V82	
	max MPa	max kN	max	min	max	max	min	max	min	min	min	max	min	max	min	
Base plate strains $\mu\text{m/m}$ ( $=10^{-6}$ )																
(2)*	28.4	316	110	-252	35	150	N/A <sup>§§</sup>	70	-295	-37	-120	139	-209	44	-127	
Std.	1.2	29.9	19	34	8	3	-	12	100	16	8	16	42	9	21	
(2)*	66.7	725	240	-616	71	376	N/A	231	-803	-78	-321	359	-444	66	-365	
Std.	1.3	65.4	11	85	7	40	-	33	47	6	12	13	17	8	41	
(1)	89	968	310	-794	59	608	N/A	332	-985	-119	-492	542	-431	56	-456	
(1)	-	-	Triggering signal missed, measured data was not available for this round.												-	-
(1)	103.6	1211	417	-973	48	783	-96	449	-838	-173	-670	645	-414	50	-449	
(5)	117.6	1397	474	-1196	93	927	-137	534	-702	-205	-751	699	-389	161	-425	
Std.	1.2	8.5	4	23	12	26	31	12	77	6	10	8	35	135	34	

Remarks:

<sup>§</sup> Measured signals of meridional strain component V81 on side of base plate cone were noisy.

<sup>§§</sup> Measured signals of tangential strain component V42 were unsettled for low pressure rounds, see figure 12.

\* Stabilizing rounds.

Table 2. Number of fired rounds in series, pressure estimate  $p_1$ , socket force component  $F_x$  and major limit value of base plate strains on sandy base for service round and overpressure round firing cases. Mean and standard deviation values are presented for the series including many rounds.

No of rds	$p_1$	$F_x$	V1	V2	V3	V41	V42	V51	V52	V61	V62	V71	V72	V81 <sup>§</sup>	V82
	max MPa	max kN	max	min	max	max	min	max	min	min	min	max	min	max	min
Base plate strains $\mu\text{m/m}$ ( $=10^{-6}$ )															
(2)*	<b>28.2</b>	<b>305</b>	<b>119</b>	<b>-209</b>	<b>50</b>	<b>151</b>	N/A <sup>§§</sup>	<b>103</b>	<b>-88</b>	<b>-42</b>	<b>-199</b>	<b>130</b>	<b>-173</b>	<b>33</b>	<b>-178</b>
Std.	0.1	10.7	29	60	12	5	-	7	25	1	54	27	6	5	33
(2)*	<b>69.2</b>	<b>746</b>	<b>228</b>	<b>-588</b>	<b>142</b>	<b>413</b>	<b>-80</b>	<b>275</b>	<b>-303</b>	<b>-117</b>	<b>-436</b>	<b>319</b>	<b>-242</b>	<b>84</b>	<b>-417</b>
Std.	0.2	34.7	13	44	8	33	2	18	29	5	52	5	18	3	59
(8)	<b>118</b>	<b>1386</b>	<b>392</b>	<b>-1013</b>	<b>99</b>	<b>913</b>	<b>-220</b>	<b>529</b>	<b>-433</b>	<b>-242</b>	<b>-825</b>	<b>703</b>	<b>-374</b>	<b>73</b>	<b>-525</b>
Std.	2.1	33.8	8	30	42	69	45	35	47	7	21	69	15	27	65
Pressure measurement breech piece was used after these rounds, socket force measurements were not available.															
(2)*	<b>72.1</b>	N/A	<b>254</b>	<b>-737</b>	<b>106</b>	<b>564</b>	<b>-169</b>	<b>348</b>	<b>-242</b>	<b>-145</b>	<b>-513</b>	<b>473</b>	<b>-251</b>	<b>30</b>	<b>-259</b>
Std.	0.2	-	7	1	2	10	0	11	5	6	9	2	2	1	19
(1)&	<b>102</b>	N/A	<b>372</b>	<b>-989</b>	<b>114</b>	<b>839</b>	<b>-260</b>	<b>517</b>	<b>-307</b>	<b>-214</b>	<b>-759</b>	<b>689</b>	<b>-340</b>	<b>35</b>	<b>-401</b>
(1)&	<b>150</b>	N/A	<b>524</b>	<b>-1427</b>	<b>169</b>	<b>1222</b>	<b>-347</b>	<b>775</b>	<b>-446</b>	<b>-320</b>	<b>-1048</b>	<b>978</b>	<b>-497</b>	<b>55</b>	<b>-629</b>
(1)&	<b>171</b>	N/A	<b>598</b>	<b>-1591</b>	<b>173</b>	<b>1376</b>	<b>-374</b>	<b>880</b>	<b>-531</b>	<b>-366</b>	<b>-1160</b>	<b>1105</b>	<b>-563</b>	<b>63</b>	<b>-722</b>
(5)	<b>188</b>	N/A	<b>622</b>	<b>-1689</b>	<b>175</b>	<b>1522</b>	<b>-404</b>	<b>1014</b>	<b>-594</b>	<b>-422</b>	<b>-1266</b>	<b>1232</b>	<b>-641</b>	<b>68</b>	<b>-871</b>
Std.	1.7	-	15	39	23	6	5	10	6	2	6	15	18	6	25

Remarks:

<sup>§</sup> Measured signals of meridional strain component V81 on side of base plate cone were noisy.

<sup>§§</sup> Measured signals of tangential strain component V42 were unsettled for low pressure rounds, see figure 12.

\* Stabilizing rounds.

& Pressure control and adjusting rounds for overpressure series.

The radial strains of inner trunk plate (V1, V3) were tension in forward and side directions and radial strain V2 was compression on the rear gauge. The tangential strains (Vx2) of trunk cone were compression in all locations due to ground pressure on the outside surfaces of the trunk cone. The meridional strains of the trunk cone plate were tension at the inner edge (V41, V51, V71), compression at the rear outer edge (V61) and tension at the side outer edge (V81). The signals of V81 strain were very noisy and unsettled.

Different behaviours of strain histories shown in figures 11 and 12 are supposed to be a consequence of nonlinear interaction between the base plate and ground base. The base plate sunk into the soil and the cavity was deeper on soft soil (sandy) than on harder soil (gravel) as shown in figure 13. However, for the strain gages where

maximum or minimum strain values were observed, it was found that sandy and gravel soil bases did not have any significant influence on the strain results as presented in data tables 1 and 2.

## Summary

It was shown that for mortar tube the use of conventional pressure estimate (Eq. 9) will lead to overestimation of pressure, pressure peak value and eventually round impulse value, if no correction methods are used. Compared to a recoiling cannon, lack of axial elastic vibration enabled the development of pressure estimate (Eq. 8). Effect of axial rigid body acceleration was analysed and its significance clearly stated. Use of pressure estimate (Eq. 8) allowed computation of results despite of direct pressure measurement failure.

Based on the measured results it was shown that transversal socket forces are insignificant compared to axial force when base plate overall strength and fatigue strength are evaluated. The earlier results show a clear difference in axial socket force between the firings on the extreme soft sandy soil and on the fixed concrete bed. Sandy and gravel soil bases didn't significantly affect the measured socket forces or major strain maximum values of base plate in this study. The difference in ground stiffness might be small even though the base plate was burrowed deeper into sandy soil than into gravel soil.

The measured data presented in this study can be used as a reference for evaluating launch cycle simulations for strength and fatigue analyses of mortar components.

## Acknowledgments

This article is based on the research study that was carried out by the order of Swedish Defence Materiel Administration (Försvarets Materielverk, FMV). The FMV's funding of the study and the permission to use the measured test firing data for preparing and publishing this article are highly acknowledged.

## References

- [1] Stanag 4110. Definition of pressure terms and their interrelationship for use in the design and proof of cannons or mortars and ammunitions. North Atlantic Treaty Organization, Standardization Agreement, Stanag.
- [2] A. Järviemi. Asepainemittausjärjestelmien vertailtavuus. Licentiate thesis. Tampere University of Technology, Tampere 2000. (in Finnish).
- [3] H. Nyberg, V.-T. Kuokkala, J. Rämö and A. Järviemi. A dynamic calibration method for crusher gauges based on material testing. *Propellants, Explosives, Pyrotechnics*, 32(1): 61-67, 2007.
- [4] H. Nyberg. Evaluation of gun propelling charge performance during the life cycle by statistical utilization of data collected in test and troop gun firings. Doctoral Dissertation. Helsinki University of Technology. Espoo 2009.

- [5] T. Erkkilä and S. Moilanen. 120 KRH:n voimamittausperäkappaleen rakenne. PvTKfys-os tutkimustodistus 686/Hi II. Ylöjärvi 1996. Confidential and unpublished research report of Finnish Defense Forces Research Centre, Physics Section. (In Finnish).
- [6] J. Merikoski and S. Moilanen. 120 KRH 93P paineputken ja peräkappaleen laukausrasitusten mittaus. PvTKfys-os tutkimustodistus 1638/Hi II. Ylöjärvi 1996. Confidential and unpublished research report of Finnish Defense Forces Research Centre, Physics Section. (In Finnish).
- [7] S. Moilanen and J. Tervokoski. Raskaan kranaatinheittimen laukauspaineen mitausmenetelmien vertailu. R. von Hertzen and T. Halme, (eds) *Proceedings of the IX Finnish Mechanics Days*. Lappeenranta University of Technology, Department of Mechanical Engineering, Report No.17: 201-213, Lappeenranta 2006. (In Finnish).
- [8] W.S. Walton. Dynamic calibration of piezoelectric chamber pressure transducers; Art, science and compromise. US Army Aberdeen Test Ctr. [https://wsmrc2vger.wsmr.army.mil/rcc/manuals/22nd\\_Transducer/File9.pdf](https://wsmrc2vger.wsmr.army.mil/rcc/manuals/22nd_Transducer/File9.pdf) (5.4.2010)
- [9] Pressure sensors for ultra-precise pressure measurement. Kistler Instrumente AG, 900-650e-04.06. <http://www.kistler.com/mediaaccess/900-650e-04.06.pdf> (5.4.2010)
- [10] Piezoelectric sensors for dynamic pressure measurements, pressure catalog. PCB Piezoelectric Inc. [http://www.pcb.com/Linked\\_Documents/Pressure/PFScat.pdf](http://www.pcb.com/Linked_Documents/Pressure/PFScat.pdf) (5.4.2010).
- [11] <http://www.hpi-gmbh.com> (17.6.2010)
- [12] P.D. Flynn. Strain gage instrumentation for a light gas gun. Frankford Arsenal Report A69-2. Philadelphia, Pa. 1969.
- [13] P.D. Flynn. Some strain-gage applications to ballistic problems. *Experimental Mechanics*; 297-304, July 1970.
- [14] P.D. Flynn. Applications of strain gages to ballistic problems. *The shock and vibration bulletin. Part 2. Structural analysis, design techniques*. The Shock and Vibration Information Center, Naval Research Laboratory. Bulletin 43, 2/4; 95-102. Washington, D.C. 1973.
- [15] P.D. Flynn. Strain-gage instrumentation for ammunition testing. *Experimental Mechanics*; 192-200, May 1975.
- [16] T.D. Andrews. Projectile driving band interactions with gun barrels. *Gun Tubes 2005 Conference. GT2005. Conference Proceedings. 10 to 13 April 2005*. Keble College Oxford. Paper S7/P28. RMCS Shrivenham 2005.
- [17] H. Keinänen, S. Moilanen, J. Toivola and J. Tervokoski. Influence of rotating band construction on gun tube loading: Numerical approach. *Gun Tubes Conference 2011, GT2011*. Paper S4/P17a. Hosted by Cranfield University at the Defence Academy of the United Kingdom, College of Management and Technology. Shrivenham. 10-12 April 2011.
- [18] J. Toivola, S. Moilanen, J. Tervokoski and H. Keinänen. Influence of rotating band construction on gun tube loading: Measurement and analysis. *Gun Tubes Conference 2011, GT2011*. Paper S4/P17b. Hosted by Cranfield University at the Defence Academy of the United Kingdom, College of Management and Technology. Shrivenham. 10-12 April 2011.

- [19] J.H. Underwood, E. Troiano and D. Crayon. Fracture Mechanics Tests and Defect Criteria for the 120-mm M121 Mortar Baseplate. US Army ARDEC, Benet Laboratories Report No. ARCCB-MR-95039, Watervliet, NY 1995.
- [20] A.G. Littlefield and J. Sibilja. Simulated proof testing of mortar baseplates. US Army RDECOM-ARDEC Benet Laboratories, Watervliet, NY 2008. Conference paper.
- [21] B.A. Boley and J.H. Weiner. Theory of Thermal Stress. Robert E. Krieger Publishing Company, Inc. Malabar, Florida. Reprint Edition 1985.

Juha Toivola  
Mekalyysi Oy  
Myllymäentie 5, FI-37960 SOTKIA, Finland  
juha.toivola(at)mekalyysi.fi

Seppo Moilanen and Henna-Riitta Jussila  
Patria Land Systems Oy  
P.O. Box 12, FI-38201 SASTAMALA, Finland  
seppo.moilanen(at)patria.fi, henna-riitta.jussila(at)patria.fi